

# A FUZZY INTEGRATED APPROACH TO IMPEDANCE CONTROL OF ROBOT MANIPULATORS

S.J.C. Marques

*Polytechnic Institute of Lisbon, Instituto Superior de Engenharia de Lisboa  
Department of Mechanical Engineering, Avenida Conselheiro Emídio Navarro, 1900 Lisboa, Portugal*

L.F. Baptista, J.M.G. Sá da Costa

*Technical University of Lisbon, Instituto Superior Técnico  
Department of Mechanical Engineering, GCAR/IDMEC, Avenida Rovisco Pais, 1049-001 Lisboa Codex, Portugal*

**Keywords:** Fuzzy adaptive control, fuzzy sliding mode control, force control, robot manipulators.

**Abstract:** This paper presents an integrated fuzzy approach to recover the performance in impedance control, reducing the errors in position and force, considering uncertainties in the parameters of the manipulator model and contact surface model. This integrated strategy considers a fuzzy adaptive compensator in the outer control loop that adjusts the manipulator tip position to compensate for uncertainties present in the environment. In the inner loop, a fuzzy sliding mode-based impedance controller compensates for uncertainties in the manipulator model, based on an inverse dynamics control law. The system error, defines the sliding surfaces of the fuzzy sliding controller as the difference between the desired and the actual impedances. In order to evaluate the force/position tracking performance and to validate the proposed control structure, simulations results are presented with a three-degree-of freedom (3-DOF) PUMA robot.

## 1 INTRODUCTION

The development of robot manipulator applications in industry to tasks that involve interaction between the en-effector and the environment, requires the development of more sophisticated force control strategies. Classical force control schemes like hybrid control (Mason, 1981) or impedance control (Hogan, 1985) are the theoretically foundation of force control strategies. However, they are not sufficient to bring robots executing tasks with interaction with a contact surface, like grinding, deburring and polishing. This lack in performance is due to variable payloads, torque disturbances, parameter variations, unmodeled robot dynamics and uncertainties in the environment parameters. Several approaches to deal with those uncertainties have been proposed, like classical adaptive control (Colbaugh et al., 1993), robust control (Liu and Goldenberg, 1991) and fuzzy adaptive control (Hsu and Fu, 1996), among others. A great research activity in force control has been registered in the last decade, however, only a few of these schemes have been implemented in experimental or industrial robots (Hsu and Fu, 2000; Baptista et al., 2001). Therefore, more sophisticated control structures are required to cope with the overall uncertainties in the force control problem.

In this paper, an integrated approach of fuzzy robust impedance and adaptive control is proposed. In this approach, an implicit force control formulation is used to compensate for uncertainties in the manipulator parameters and the contact surface model. The fuzzy adaptive controller corrects the reference position to a fuzzy robust impedance controller in the inner control loop. This controller includes a fuzzy sliding mode term, where a new sliding surface is defined, based on the impedance error. In the proposed approach, the impedance controller design is equivalent to the sliding mode controller design.

The outline of the paper is as follows: section 2 presents a brief description of the manipulator dynamics in the constrained coordinate frame. Section 3 presents the overall force control structure and a brief description of the two control schemes. Simulation results are presented in Section 4, and finally in Section 5 some conclusions are drawn.

## 2 ROBOT DYNAMICS AND ENVIRONMENT

Let's consider an  $n$ -link rigid-joint robot manipulator constrained by contact with the environment.

The complete dynamic model in cartesian space is described by:

$$\mathbf{H}_x(\mathbf{x})\ddot{\mathbf{x}} + \mathbf{h}_x(\mathbf{x}, \dot{\mathbf{x}}) = \mathbf{u} - \mathbf{f}_e \quad (1)$$

The vectors  $\mathbf{x}$ ,  $\mathbf{u}$  and  $\mathbf{f}_e \in \mathbb{R}^n$  ( $n \times 1$ ) represent the end-effector position in the suitable reference coordinate frame, the force control signal, and the force exerted by the manipulator on the environment, respectively. The term  $\mathbf{h}_x$  is given by  $\mathbf{C}_x(\mathbf{x}, \dot{\mathbf{x}})\dot{\mathbf{x}} + \mathbf{g}_x(\mathbf{x}) + \mathbf{d}_x(\dot{\mathbf{x}})$ , where  $\mathbf{C}_x(\mathbf{x}, \dot{\mathbf{x}})$ ,  $\mathbf{g}_x(\mathbf{x})$  and  $\mathbf{d}_x(\dot{\mathbf{x}})$  are the Coriolis matrix, gravity and friction vectors, respectively. Generally, a task frame attached to the constrained surface is selected, when the robot manipulator tip moves in a force control task, so as to easily describe the desired position  $\mathbf{x}_d$  and force  $\mathbf{f}_d$  trajectories. The internal joint coordinates  $\mathbf{q}$ ,  $\dot{\mathbf{q}}$  and  $\ddot{\mathbf{q}}$  must be transformed in external cartesian ones  $\mathbf{x}$ ,  $\dot{\mathbf{x}}$  and  $\ddot{\mathbf{x}}$ , by means of the forward kinematics, where  $\mathbf{x}$  is the position of the tip manipulator in the task frame coordinates. Regarding the external forces, let's decompose the force vector  $\mathbf{f}_e$ , given by the force sensor in all of its components and already transformed in the task frame: a normal component  $f_n$  in the perpendicular direction to the surface environment and a tangential component  $f_t$ , in the velocity tip manipulator direction. Let's also assume that the friction coefficient  $\mu$  between the manipulator tip and the environment is known. Thus, it is possible to calculate exactly the perpendicular direction  $\hat{\mathbf{n}}$  to the environment surface, implicitly given by the force sensor. Thus, without loss of generality, only three elements in force and position,  $\mathbf{f}_e$  and  $\mathbf{x}$ , defined in its components as  $\mathbf{f}_e = [f_n, f_t, 0]^T$  and  $\mathbf{x} = [x_1, x_2, x_3]^T$ , respectively, are going to be considered. The force control is exerted along the first component and the position control is done on the other two components. In what concerns the environment characteristics, several models have been proposed, based on elementary mechanic components (spring, dump and mass), with one or two degree of freedom (Epping and Seering, 1987). In this article, the environment is modelled as a spring mechanical element with stiffness coefficient  $k_e$ .

### 3 THE OVERALL CONTROL STRUCTURE

The proposed control structure can be defined as a position based explicit force control, such that in the inner loop a position based controller is feeded, in part, with position errors by a controller in the external loop (Fig. 1).

In the external loop, the controller is of fuzzy adaptive type, which transforms the force error in a position adjustment. The main objective of the fuzzy

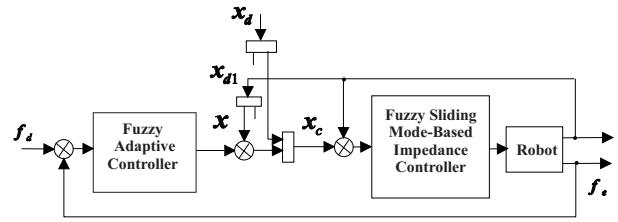


Figure 1: Block diagram of the overall control structure.

adaptive controller is to compensate environment uncertainties, like stiffness and geometric location. As referred above, the fuzzy adaptive controller feeds in part the inner position controller, because it corrects only the manipulator tip position  $x_1$  in the perpendicular direction to the contact surface, based on the force error  $e_f$ . Moreover, the inner position controller will compensate for uncertainties in the manipulator dynamic model. The inner position controller, is a fuzzy sliding mode-based impedance algorithm, with an inverse dynamics control law. As the dynamic model of the manipulator is not exactly known, an impedance error will appear. This impedance error defines a sliding surface, which, when the system is in sliding mode, after it has reached the surface, the state trajectory continues to be on it.

#### 3.1 Fuzzy sliding mode-based impedance controller

Let's consider the following impedance control law:

$$\begin{aligned} \boldsymbol{\sigma} = & \mathbf{M}_d(\ddot{\mathbf{x}}_d - \ddot{\mathbf{x}}) + \mathbf{B}_d(\dot{\mathbf{x}}_d - \dot{\mathbf{x}}) + \\ & \mathbf{K}_d(\mathbf{x}_d - \mathbf{x}) - \mathbf{f}_e, \end{aligned} \quad (2)$$

where  $\mathbf{M}_d$ ,  $\mathbf{B}_d$  and  $\mathbf{K}_d$  are the inertial, damping and stiffness positive definite matrices, respectively, and  $\mathbf{x}_d$  is the desired position. The second term in (2) vanishes when no uncertainties are present in the manipulator dynamic model. When uncertainties are considered, the second member in (2) assumes a value with some norm different from zero. As  $\boldsymbol{\sigma} = \mathbf{0}$  does not represent a manifold in the state space  $(\mathbf{x}, \dot{\mathbf{x}})$ , integrating  $\boldsymbol{\sigma}$  a sliding surface  $s = \mathbf{0}$ , can be defined as (Lu and Goldenberg, 1995):

$$\begin{aligned} s = & \dot{\mathbf{x}} - \dot{\mathbf{x}}_d + \mathbf{M}_d^{-1}\mathbf{B}_d(\mathbf{x} - \mathbf{x}_d) + \mathbf{M}_d^{-1} \int_0^t \mathbf{f}_e d\tau \\ & + \mathbf{M}_d^{-1}\mathbf{K}_d \int_0^t (\mathbf{x} - \mathbf{x}_d) d\tau \end{aligned} \quad (3)$$

When the system is in sliding mode, after it has reached the surface, the state trajectory continues to be on the sliding surface ( $s = \mathbf{0}$ ) so that ( $\dot{s} = \mathbf{0}$ ) and  $\boldsymbol{\sigma} = -\mathbf{M}_d\dot{s} = \mathbf{0}$  is obtained. This indicates that

the impedance controller design is equivalent to design a sliding mode controller which guarantees that the state trajectory reaches the sliding surface and remains on it, thereafter. The norm of  $\sigma$  is used to represent the deviation of the system state from the sliding surface. This deviation reflects the impedance control error.

Let's consider also an inverse dynamics control law, based on the robot nominal dynamics:

$$\mathbf{u} = \widehat{\mathbf{H}}_x(\mathbf{x})\ddot{\mathbf{x}}_s + \widehat{\mathbf{h}}_x(\mathbf{x}, \dot{\mathbf{x}}, \dot{\mathbf{x}}_s) + \mathbf{f}_e - \mathbf{K}_{fz}, \quad (4)$$

where

$$\widehat{\mathbf{h}}_x(\mathbf{x}, \dot{\mathbf{x}}, \dot{\mathbf{x}}_s) = \widehat{\mathbf{C}}_x(\mathbf{x}, \dot{\mathbf{x}})\dot{\mathbf{x}}_s + \widehat{\mathbf{g}}_x(\mathbf{x}) + \widehat{\mathbf{d}}_x(\dot{\mathbf{x}}) \quad (5)$$

The velocity  $\dot{\mathbf{x}}_s$  in (4) and (5), is defined as:

$$\begin{aligned} \dot{\mathbf{x}}_s = & \dot{\mathbf{x}}_d - \mathbf{M}_d^{-1}\mathbf{B}_d(\mathbf{x} - \mathbf{x}_d) - \mathbf{M}_d^{-1}\int_0^t \mathbf{f}_e d\tau \\ & - \mathbf{M}_d^{-1}\mathbf{K}_d \int_0^t (\mathbf{x} - \mathbf{x}_d) d\tau \end{aligned} \quad (6)$$

From (3) and (6) the relation  $\dot{\mathbf{x}}_s = \dot{\mathbf{x}} - \mathbf{s}$  holds, which means that when the state trajectory is on the sliding surface, the actual velocity  $\dot{\mathbf{x}}$  follows  $\dot{\mathbf{x}}_s$  exactly. The term  $\mathbf{K}_{fz}$  is given by:

$$\mathbf{K}_{fz} = \mathbf{K}_v \times \mathbf{u}_{fz}, \quad (7)$$

where  $\mathbf{K}_v$  is a diagonal matrix of control gains based on the upper bounds of the uncertainties in the dynamic model and  $\mathbf{u}_{fz}$  is a fuzzy system (Lu and Goldenberg, 1995). This fuzzy system is a counterpart of the Sliding Mode Controller with Boundary Layer (SMC-BL). In the boundary layer (BL), near the sliding line  $s = 0$ , the control input dynamics is smoothed, avoiding the chattering effects, ensuring that the error states remain within the layer. Inside this BL, a null control signal along the switching line is verified, and increases the absolute value of the control signal, as the error states are far away from the switching line. A fuzzy system with a diagonal form rule base considering the error and its derivative as inputs, has a similar behavior to the above prescribed in (Palm et al., 1997). However, this rule base can be reformulated as one input one output, with the input variable  $s$  inside the BL and the output variable  $u$ , accordingly Table 1 and regarding the following rule:

$$\begin{aligned} R_1 : & \quad \text{IF } \tilde{s} \text{ is } \text{Negative High} \\ & \quad \text{THEN } \tilde{u} \text{ must be } \text{Negative High} \end{aligned}$$

This rule base reduces the number of fuzzy rule control and can assume a more general behavior than the SMC-BL. In the SMC-BL with boundary layer thickness  $\phi$ , the control signal  $u$  is basically given by:

$$u = k \times \text{sat}\left(\frac{s}{\phi}\right) \quad (8)$$

Table 1: Reformulated rule base of a fuzzy sliding mode controller with input  $\tilde{s}$  and output  $\tilde{u}$ . (P-Positive, N-Negative, ZE-Zero, L-Low, M-Medium and H-High)

| $\tilde{s}$ | NH | NM | NL | ZE | PL | PM | PH |
|-------------|----|----|----|----|----|----|----|
| $\tilde{u}$ | NH | NM | NL | ZE | PL | PM | PH |

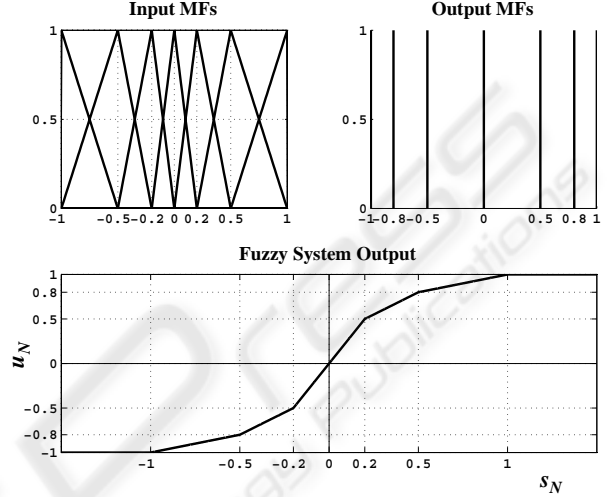


Figure 2: Input and output membership functions and output of the fuzzy system.

This control assumes a linear transfer characteristic inside the BL. In the FSMC reformulated in that way, using for instance triangular membership functions with fuzzy partition leads to stretching the centers of the input variable towards the origin and expanding the centers of the output variable towards the extremes. The resulting output of the fuzzy system is a transfer characteristic with different slopes, which is greater than 1 near the origin and decreases towards the extremes, where it is less than 1. This is shown in Fig. 2, where the input and output are normalized into the interval  $[-1, 1]$  and different  $\phi_i$  such that  $\sum \phi_i = \phi$ , that defines the tracking quality. The resulting transfer characteristic achieved by this way must be chosen if for small errors the system is supposed to be more sensitive to disturbances and fast responses where the error states are near the origin. As the input of the reformulated FSMC is the variable  $s$ , inside the BL with thickness  $\phi$ , this can be implemented with the input  $\text{sat}(\frac{s}{\phi})$ , which results in the normalized interval  $[-1, 1]$  by self. This is the same as the input variable  $s$  with  $\frac{1}{\phi}$  as the scaling factor of the input variable considering the same normalized interval. The output of the fuzzy system is inside the interval  $[-1, 1]$ , which will be scaled by the elements of the matrix  $\mathbf{K}_v$  given in (7).

### 3.2 Fuzzy adaptive controller

The overall fuzzy adaptive control scheme (FAC) presented in this paper, based on the Fuzzy Model Reference Learning Controller (Layne and Passino, 1996), is shown in Fig. 3.

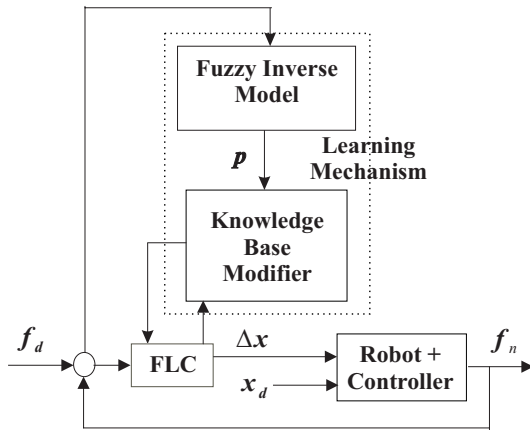


Figure 3: Fuzzy adaptive control scheme (FAC).

The FAC is mainly based on the Fuzzy Logic Controller (FLC), and the learning mechanism. The FLC is adapted in the membership functions of its consequents by the learning mechanism. The FLC inputs are the force error  $e_f(kT) = f_d(kT) - f_n(kT)$  and its finite difference  $\Delta e_f(kT) = e_f(kT) - e_f(kT - T)$  or the trapezoidal area of the force error  $\delta e_f(kT) = \frac{e_f(kT) + e_f(kT - T)}{2} T$ . The learning mechanism is composed by the fuzzy inverse model and the knowledge-base modifier. The fuzzy inverse model attempts to characterize approximately the representation of the inverse dynamics of the environment. This is called by fuzzy inverse model that maps the error in the output variables and possibly other parameters such as the functions of the error and the process operating conditions, to the necessary changes in the input process (Layne and Passino, 1996). The fuzzy inverse model is designed to adjust the manipulator tip position in the perpendicular direction to the environment surface to compel the force  $f_n(kT)$  exerted on it, to be as close as possible to  $f_d(kT)$ . The knowledge base modifier performs the function of modifying the fuzzy controller, in order to improve the robot's performance. Based on the necessary changes given by the output of the fuzzy inverse model  $p(kT)$ , the knowledge base modifier changes the membership functions of the FLC consequents, only for those whose activation level  $\delta_{ij}$  are greater than zero at the instant  $(kT - T)$ . All others remain unchanged. This

can be formulated as:

$$C_{ij}(kT) = C_{ij}(kT - T) + p(kT) \quad \text{if } \delta_{ij}(kT - T) > 0; \quad (9)$$

and

$$C_{ij}(kT) = C_{ij}(kT - T) \quad \text{if } \delta_{ij}(kT - T) = 0 \quad (10)$$

As shown in (Layne and Passino, 1996), the FAC output that would have been desired, is expressed by:

$$\Delta x^*(kT - T) = \Delta x(kT - T) + p(kT) \quad (11)$$

In the inner position control loop, the FSMC follows the reference or commanded positions and velocities, given by the path planning algorithm in the position controlled directions. In the force controlled direction, those commanded position and velocity are given by the FAC algorithm. In the last controlled direction, representing the position and velocity as a two component vector  $x_c = [x_c \dot{x}_c]^T$ , the element  $x_c$  is given by:

$$x_c = x + u_{FAC}, \quad (12)$$

where  $x$  is the actual tip position manipulator and  $u_{FAC}$  is the FAC output. In order to compute the sliding variable along this direction, the vector  $[e_x \dot{e}_x]^T$  is given by:

$$[e_x \dot{e}_x]^T = x - x_c = -[u_{FAC} \dot{u}_{FAC}]^T \quad (13)$$

## 4 SIMULATION RESULTS

The overall force/position control structure described in Section 3 is now applied, by simulation, to a 3-DOF PUMA 560 robot model, that executes a trajectory along a flat surface, as shown in Figure 4. To simulate uncertainties in the environment geometry, a mismatch of about  $15^\circ$  between the planned and the actual plane is imposed. The simulation environment incorporates the model of the robot, as described in (Corke, 1996), including the nonlinear arm dynamics and joint friction, providing the basis for a realistic evaluation of the controller performance. The control scheme applied to the robot dynamic model used in this study, was implemented in the MATLAB/SIMULINK environment, using the Runge-Kutta fourth order integration method. The control laws applied to the manipulator model were implemented with a sampling frequency of 1 kHz. The inverse dynamics control law of the manipulator only consider the diagonal terms of the inertial matrix and the gravitational terms, as shown in Eq. (14):

$$\begin{bmatrix} \tau_1 \\ \tau_2 \\ \tau_3 \end{bmatrix} = \begin{bmatrix} \hat{H}_{1,1} & 0 & 0 \\ 0 & \hat{H}_{2,2} & 0 \\ 0 & 0 & \hat{H}_{3,3} \end{bmatrix} + \begin{bmatrix} \hat{g}_1 \\ \hat{g}_2 \\ \hat{g}_3 \end{bmatrix} \quad (14)$$

For robustness analysis, the inertial parameters, like link masses and moments of inertia are disturbed between 10% and 30% from its nominal value. The desired force path is represented in Fig. 5(a) and the stiffness coefficient of the environment varies along time, accordingly Fig. 5(b).

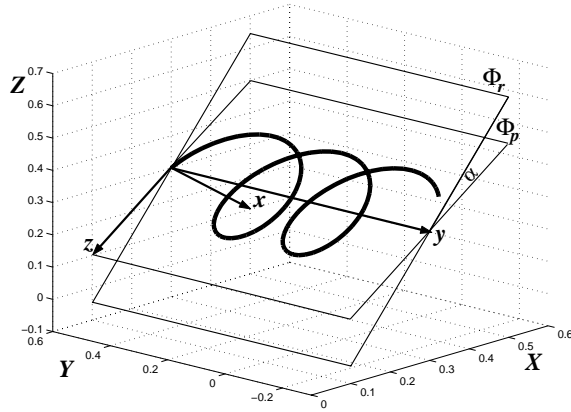


Figure 4: Trajectory of the 3-DOF PUMA manipulator.

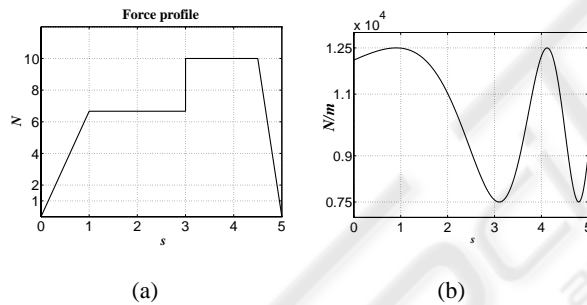


Figure 5: a) Desired force profile. b) Environment stiffness.

Table 2: Rule base of the fuzzy inverse model.

| $\tilde{e}_f \setminus \tilde{\Delta e}_f$ | NH | NM | NL | Z  | PL | PM | PH |
|--|----|----|----|----|----|----|----|
| PH   | Z  | Z  | PL | PL | PM | PH | PH |
| PM   | NL | Z  | PL | PL | PM | PM | PH |
| PL   | NM | NL | Z  | PL | PL | PH | PH |
| Z  | NH | NM | NL | Z  | PL | PM | PH |
| NL   | NH | NM | NL | NL | Z  | PL | PM |
| NM   | NH | NM | NM | NL | NL | Z  | PL |
| NH   | NH | NH | NM | NL | NL | Z  | Z  |

It is assumed that the manipulator is already in contact with the surface and the end-effector always maintains contact with the environment during the execution of the task. The impedance matrices have the following values:  $M_d =$

Table 3: Rule base of the FLC.

| $\tilde{e}_f \setminus \tilde{\Delta e}_f$ | N        | Z        | P        |
|--|----------|----------|----------|
| P  | $C_{11}$ | $C_{12}$ | $C_{13}$ |
| Z  | $C_{21}$ | $C_{22}$ | $C_{23}$ |
| N  | $C_{31}$ | $C_{32}$ | $C_{33}$ |

$diag(5, 5, 5)$ ,  $B_d = diag(316, 141, 141)$  and  $K_d = diag(5000, 1000, 1000)$ . The boundary layer thickness for the three subsystems at the fuzzy sliding mode controller was setting as  $\Phi = diag(0.05, 0.05, 0.05)$  and the matrix  $K_v$  in (7) is  $K_v = diag(50, 20, 20)$  for the three orthogonal directions. Also, the transfer characteristic inside the boundary layer as presented in Fig. 2 is used, which reveal an increasing velocity response. The rule base of the fuzzy inverse model is presented on Table 2 and the rule base of the FLC has nine rules, accordingly to Table 3. The centers  $C_{ij}$  are adapted by the learning mechanism. It is also assumed that the inputs to the fuzzy inverse model and to the FLC algorithm are the same: the force error  $e_f$  and its difference  $\Delta e_f$ . The scaling factors to the fuzzy inverse model are  $[8 \ 6; 0.25]$  and  $[6 \ 6; 0.0005]$  for the FLC. All the fuzzy systems are Takagi-Sugeno type (Palm et al., 1997), with a fuzzy partition at the antecedents, trapezoidal shape and singletons  $C_{ij}$  at the consequents. The simulation results can be observed in Figs. 6, 7 and 8. In Fig. 6 joint torques, tip position and force errors are presented without compensation. It can be observed that the performance is greatly reduced. In Fig. 7 both fuzzy adaptive and fuzzy sliding controllers compensate for the uncertainties, recovering the performance of the impedance control. In Fig. 8 the adjustment activity of the FLC consequents, done by the learning mechanism in order to compensate for uncertainties in the environment, is shown.

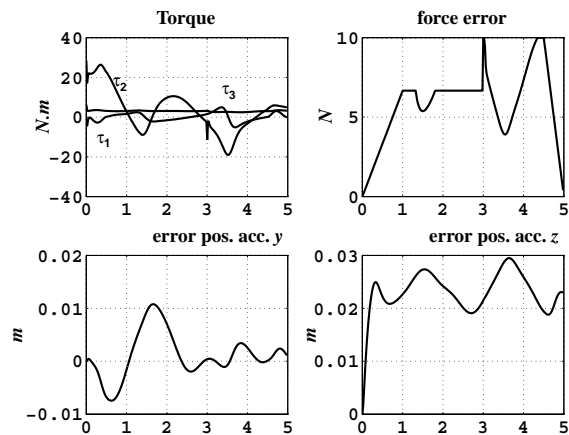


Figure 6: Simulation results without compensation.

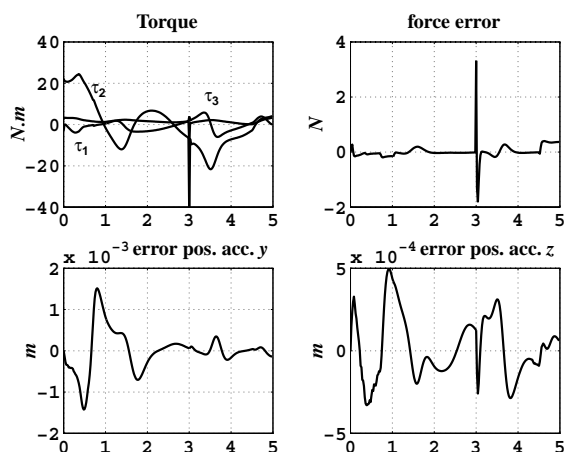


Figure 7: Simulation results with compensation of uncertainties in environment and robot dynamic model.

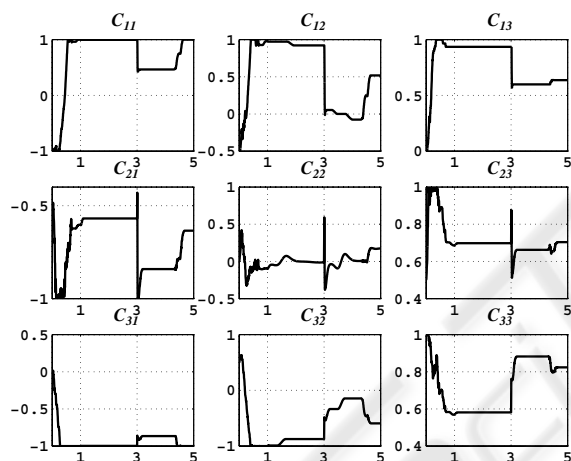


Figure 8: The adaptation of the consequents of the FLC membership functions.

## 5 CONCLUSIONS

In this article, an integration of fuzzy adaptive and fuzzy robust force/position control to compensate for overall uncertainties, considering an impedance control formulation, is presented. The tip position adjusted by the fuzzy adaptive controller in the perpendicular direction to the surface, to compensate for uncertainties in the environment is feeded to an inner position controller. This controller is a fuzzy sliding mode-based impedance control that compensates for uncertainties in the manipulator dynamic model. The adjustment in position done by the fuzzy adaptive controller, based on the force error and the effort done by the fuzzy sliding mode-based impedance controller in the inner loop, recovers the impedance control performance and reduces the errors in position

and force. This control structure also exhibits a good performance considering nonrigid materials with uncertainties.

Future work will concentrate on the implementation of this control structure on a industrial PUMA 562 robot.

## ACKNOWLEDGEMENTS

This research was partially supported by program POCTI, FCT, Ministério da Ciência e do Ensino Superior, Portugal

## REFERENCES

Baptista, L., Sousa, J., and Sá da Costa, J. G. (2001). Fuzzy predictive algorithms applied to real-time force control. *Control Engineering Practice*, 9(4):411–423.

Colbaugh, R., Seraji, H., and Glass, K. (1993). Direct adaptive impedance control of robot manipulators. *Journal of Robotic Systems*, 10:217–242.

Corke, P. (1996). A robotics toolbox for MATLAB. *IEEE Robotics and Automation Magazine*, 3(1):24–32.

Epping, S. D. and Seering, W. P. (1987). Introduction to dynamic models for robot force control. *IEEE Control Systems Magazine*, pages 48–51.

Hogan, N. (1985). Impedance control: an approach to manipulation: Part I-II-III. *Journal of Dynamic Systems, Measurement, and Control*, 107:1–24.

Hsu, F.-Y. and Fu, L.-C. (1996). Adaptive fuzzy hybrid force/position control for robot manipulators following contours of an uncertain object. *Proc. IEEE International Conference on Robotics and Automation*.

Hsu, F.-Y. and Fu, L.-C. (2000). Intelligent robot deburring using adaptive fuzzy hybrid position/force control. *IEEE Transactions on Robotics and Automation*, 16(4):325–335.

Layne, J. and Passino, K. M. (1996). Fuzzy model reference learning control. *Journal of Intelligent and Fuzzy Systems*, 4:33–47.

Liu, G. J. and Goldenberg, A. A. (1991). Robust hybrid impedance control of robot manipulators. *Proc. IEEE International Conference on Robotics and Automation*.

Lu, Z. and Goldenberg, A. A. (1995). Robust impedance control and force regulation: Theory and experiments. *International Journal of Robotics Research*, 14-3:225–254.

Mason, M. (1981). Compliance and force control for computer controlled manipulators. *IEEE Transactions on Systems, Man and Cybernetics*, 11(6):418–432.

Palm, R., Driankov, D., and Hans, H. (1997). *Model Based Fuzzy Control*. Springer-Verlag, Berlin Heidelberg.